Available online at www.sciencedirect.com
ScienceDirect
Journal of Solid State Chemistry 180 (2007) 1889–1893
JOURNAL OF SOLID STATE CHEMISTRY
www.elsevier.com/locate/jssc

Synthesis and crystal structure of $LiBa_2N$ and identification of $LiBa_3N$

Volodymyr Smetana[a], Volodymyr Babizhetskyy[a], Grigori V. Vajenine[a,b], Arndt Simon[a,*]

[a]*Max-Planck-Institut für Festkörperforschung, Heisenbergstrasse 1, D-70569 Stuttgart, Germany*
[b]*Institut für Anorganische Chemie, Universität Stuttgart, Pfaffenwaldring 55, D-70569 Stuttgart, Germany*

Received 16 March 2007; received in revised form 20 April 2007; accepted 25 April 2007
Available online 1 May 2007

Abstract

The metal-rich part of the Li–Ba–N system was investigated using powder and single-crystal X-ray diffraction analysis. The crystal structures of two new ternary subnitrides, $LiBa_2N$ and of $LiBa_3N$, were determined from single-crystal and powder X-ray diffraction data, respectively. $LiBa_2N$ has a tetragonal structure (space group, $P4_2/nmc$, $Z = 8$, $a = 7.980(1)$, $c = 14.263(2)$ Å). The structure contains infinite mutually perpendicular rows of edge-sharing $LiBa_5N$ octahedra. $LiBa_3N$ is isostructural with $NaBa_3N$ ($P6_3/mmc$, $Z = 2$, $a = 8.182(1)$, $c = 6.922(4)$ Å).

Keywords: Subnitride; Barium; Lithium; X-ray diffraction

1. Introduction

In recent years novel subnitrides of alkaline-earth metals and of Ba together with Na were discovered [1]. First M_2N [2] (M = Ca, Sr and Ba), then $NaBa_3N$ [3], Na_5Ba_3N [4], and $Na_{16}Ba_6N$ [5], and a series of compounds with the general composition $Na_nBa_{14}CaN_6$ ($n = 7$, 8, 14, 17, 21, 22) [6–8] became known. Their structures contain discrete or condensed Ba_6N octahedra; in $Na_nBa_{14}CaN_6$ the large cluster $Ba_{14}CaN_6$ occurs. A general feature is strong ionic bonding within the clusters and metallic bonding in the space between them. Attempts to prepare corresponding phases with the heavier alkali metals, K, Rb, Cs were unsuccessful, not unexpected due to the poor miscibility of Ba with these elements. On the other hand, Li and Ba form two binary intermetallic compounds, $BaLi_4$ [9] and $Ba_{19}Li_{44}$ [10], and the Li–Ba system could therefore be a good candidate for subnitride formation. Our discovery of the first such compound, $Li_{80}Ba_{39}N_9$ [11], prompted a more detailed investigation of the Li–Ba–N system.

2. Experimental section

2.1. Reagents

Ba metal (Merck, 99%, distilled twice with intermediate heating in a closed tantalum container at 1200 K in vacuum to remove hydrogen), Li metal (Merck, 99.5%), Li_3N (Alfa Aesar, 99.5%), $Ba(N_3)_2$ (Schuchardt, 98.5%, recrystallized and dried under vacuum), Ba_2N obtained by the reaction of Ba metal with $Ba(N_3)_2$ at 450 °C (purity was checked with powder X-ray diffraction analysis) were used for syntheses.

2.2. Syntheses

Due to the extreme sensitivity of the reagents and products to air, all handling was performed under purified argon using Schlenk technique or a glove box (Ar 99.9%, molecular sieve, $H_2O < 0.1$ ppm; $O_2 < 0.05$ ppm). All reactions were carried out in closed Ta ampoules, which were arc-welded and sealed inside Solidex glass ampoules. The Ta ampoules had previously been cleaned in a mixture of concentrated HNO_3 and HF (85:15 by volume).

*Corresponding author. Fax: +49 711 689 1642.
E-mail address: a.simon@fkf.mpg.de (A. Simon).

0022-4596/$ - see front matter © 2007 Elsevier Inc. All rights reserved.
doi:10.1016/j.jssc.2007.04.012

$LiBa_2N$: The starting materials Ba_2N (0.572 g, 1.98 mmol) and Li (0.0138 g, 1.98 mmol) were enclosed in a Ta ampoule in an argon atmosphere. The reaction mixture was heated to 420 °C at a rate of 10 °C h^{-1} and kept at this temperature for 10 days. Then it was cooled to 200 °C at 2 °C h^{-1} and annealed at this temperature for 1 month. The resulting product consisted of approx. 20 wt% of $LiBa_2N$ together with Ba_2N and $LiBa_3N$ according to powder X-ray diffraction analysis. Single crystals of $LiBa_2N$ were also obtained in an attempt to prepare another Li–Ba subnitride, $LiBa_3N$.

$LiBa_3N$: Ba (0.5667 g, 4.1 mmol), $Ba(N_3)_2$ (0.0537 g, 0.24 mmol) and Li (0.0102 g, 1.45 mmol) were mixed and enclosed in a Ta ampoule (glove box, Ar atmosphere). To decompose the azide, the sample was heated to 400 °C within 20 h and held at this temperature for 70 h. Then the sample was slowly (1 °C h^{-1}) cooled to 120 °C and annealed at this temperature for 2 months. During investigation of the Li–Ba–N system, $LiBa_3N$ was obtained in several two- or three-phase samples together with all other Ba or Li–Ba subnitrides (Ba_2N, Ba_3N, $Li_{80}Ba_{39}N_9$, and $LiBa_2N$) and also with Ba, Li and Li_3N.

2.3. X-ray diffraction and structure refinement

Single crystals of $LiBa_2N$ were sealed under argon atmosphere in glass capillaries for X-ray investigation. Single-crystal diffraction data were collected at room temperature using a STOE IPDS I diffractometer with AgK_α radiation by oscillation of the crystal around the ω axis. The starting atomic parameters derived via direct methods using the program SIR 97 [12] were subsequently refined in the space group $P4_2/nmc$ with the program SHELX-97 [13] (full-matrix least-squares on F^2 with anisotropic atomic displacement parameters for all atoms) within the WinGX program package [14].

X-ray powder diffraction patterns were obtained on a powder diffractometer STOE STADI P with $MoK_{\alpha1}$ radiation, using capillaries sealed under dried argon to avoid oxidation. The unit cell parameters for $LiBa_3N$ were refined with the help of the WinCSD program package [15] from powder data as $a = 8.182(1)$, $c = 6.922(4)$ Å. Silicon (6N, $a_{Si} = 5.43102$ Å) was used as an external standard. Temperature-dependent investigations were also performed on a Guinier–Simon camera [16] with $CuK_{\alpha1}$ radiation.

2.4. Thermal analysis

All thermal analyses were performed with sample amounts of 20–40 mg in an argon atmosphere. Laser-welded tantalum ampoules (diameter 2 mm, length approx. 15 mm) and Pt–PtRh thermocouple thermocoax were used in a home-made device throughout this investigation. The temperature was recorded with a sensitive micro-voltmeter Hewlett Packard 3457A, calibration was performed and frequently checked by measuring the extrapolated onset temperatures of the last phase transition (125 °C) and melting (170 °C) peaks of NH_4NO_3, or phase transition and melting peaks of KNO_3, 128 and 337 °C, respectively. The samples were heated to 300–600 °C with a rate of 3 °C min^{-1} and cooled with 1 °C min^{-1}.

2.5. Theoretical studies

Band structure calculations were carried out at the DFT level using the full-potential LAPW method implemented in the WIEN2k package (version 06) [17] with the Perdew–Burke–Ernzerhof GGA exchange correlation potential [18]. The energy cutoff between the core and valence states was lowered to −8 Ry in order to include Ba 4*d* states as semi-core levels. Calculations were run with 72 *k*-points in the irreducible wedge of the Brillouin zone. The geometry was optimized by minimizing the total energy as a function of the unit cell volume and c/a ratio combined with the optimization of the only internal structural parameter x_{Ba}. The calculated band structure for $NaBa_3N$ (not shown here) is similar to that obtained in an earlier study [19] for the metal-based bands. The top of the filled nitrogen-based bands was found to lie higher in energy but still well below the Fermi level at −1.6 eV.

3. Results and discussion

3.1. Crystal structures

The metal-rich part of the Li–Ba–N system was investigated, and two new compounds were found. The crystal structure of $LiBa_2N$ was determined from

Table 1
Details of the crystal structure investigation for $LiBa_2N$

Empirical formula	$LiBa_2N$
Formula weight	295.56
Temperature, K	293
Wavelength, Å	0.56086
Crystal system	Tetragonal
Space group	$P4_2/nmc$
a, Å	7.980(1)
c, Å	14.263(2)
Volume, Å^3	908.3(9)
Z	8
Density (calculated), g/cm^3	4.323
μ, mm^{-1}	9.010
F(0 0 0)	972
Index ranges	$-13 \leqslant h \leqslant 13$
	$-13 \leqslant k \leqslant 13$
	$-23 \leqslant l \leqslant 23$
Reflections collected	30,260
Independent reflections	1216
Refinement method	Full-matrix least-squares on F^2
Data/restraints/parameters	1216/0/26
Goodness-of-fit on F^2	1.02
Final *R* indices $[I > 2\sigma(I)]^a$	$R_1 = 0.039$, w$R_2 = 0.077$
R indices (all data)	$R_1 = 0.071$, w$R_2 = 0.088$
Largest diff. peak and hole, ē/Å^3	2.16 and −2.34

single-crystal data, and that of $LiBa_3N$ by analyzing powder X-ray diffraction data. Details of the data collection and structure refinement of $LiBa_2N$ are listed in Table 1. Positional, anisotropic displacement parameters, and relevant interatomic distances are given in Tables 2–4, respectively.

$LiBa_2N$ crystallizes in a new structure type of tetragonal symmetry with a small unit cell. Edge-sharing N-centered $LiBa_5$ octahedra form orthogonal rows (Fig. 1). Each of these octahedra has common edges with four other according to $LiBa_{2/2}Ba_{3/3}N$. Groups of four face-sharing $LiBa_5N$ octahedra are joined to the new cluster $Li_4Ba_{8/2}Ba_4N_4$ (Fig. 2a) with a Ba_4N_4 heterocubane-like core (Fig. 2b) and $Ba_{2/2}Li$ triangles above all N atoms. In comparison, the discrete $Ba_{14}CaN_6$ clusters in $Na_nBa_{14}CaN_6$ are built from six face-sharing Ba_5CaN octahedra. In the $Li_4Ba_{8/2}Ba_4N_4$ unit (as in the $Ba_{14}CaN_6$ cluster) there are two inequivalent positions of Ba atoms. One Ba has contacts with three N atoms, and the second only with two.

Rows of edge-sharing N- or O-centered polyhedra are also known for other metal-rich Ba compounds, those with edge-sharing Ba_6N octahedra in the Ba subnitride Ba_2N[2] and with edge-sharing Ba_4O tetrahedra in the Na–Ba suboxide $NaBa_2O$ [20]. In $NaBa_2O$, unlike in the present compound, there are only Ba–O contacts with Na filling the rest of space. Interestingly, the structure of $LiBa_2N$ can be derived from a bcc packing of metal atoms almost in the

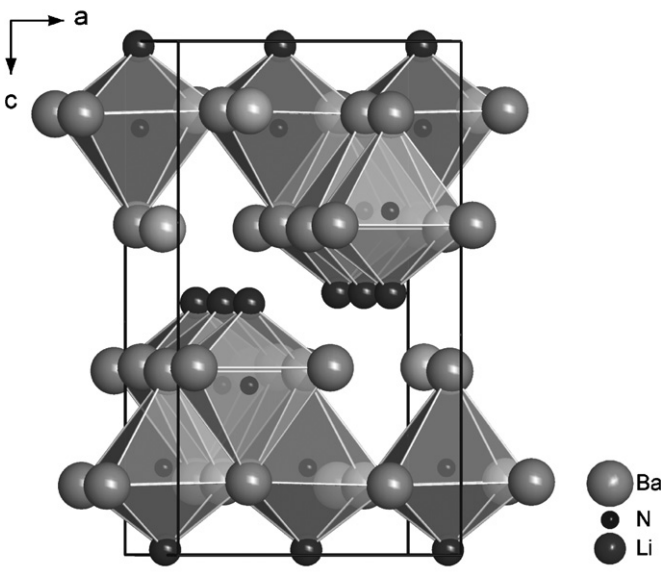

Fig. 1. Tetragonal unit cell of $LiBa_2N$.

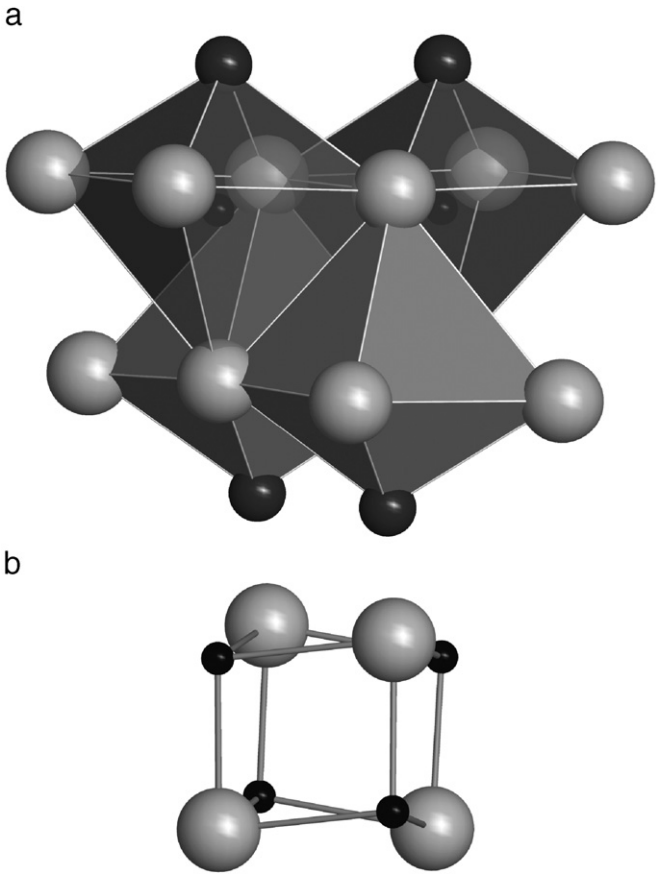

Fig. 2. (a) $Li_4Ba_4Ba_{8/2}N_4$ cluster in the structure of $LiBa_2N$, (b) heterocubane-type Ba_4N_4 core.

Table 2
Atomic coordinates and equivalent/isotropic thermal displacement parameters for $LiBa_2N$

Atom	Position	x	y	z	$U_{eq/iso}$, Å^2
Li1	8*g*	3/4	0.998(4)	0.991(1)	0.026(4)
Ba1	8*g*	3/4	0.0070(1)	0.14241(3)	0.0136(1)
Ba2	8*g*	3/4	0.9908(1)	0.86504(3)	0.0149(1)
N1	8*g*	3/4	0.004(1)	0.8311(8)	0.032(2)

Table 3
Anisotropic displacement parameters[a] for $LiBa_2N$

Atom	U_{11}	U_{22}	U_{33}	U_{23}
Li1	0.014(14)	0.002(11)	0.061(11)	0.011(7)
Ba1	0.0121(3)	0.0179(3)	0.0109(2)	−0.0026(2)
Ba2	0.0238(4)	0.0108(3)	0.0100(2)	−0.0004(2)
N1	0.021(5)	0.031(5)	0.044(5)	0.003(4)

[a] $U_{13} = U_{12} = 0$.

Table 4
Selected interatomic distances in the structure of $LiBa_2N$

Atoms	Distance (Å)	Atoms	Distance (Å)
N1–Ba1	2.69(1)	Ba1–Ba2 × 2	3.991(2)
N1–Ba1 × 2	2.833(8)	Ba1–Ba2	3.958(1)
N1–Ba2 × 2	2.788(8)	Ba1–Ba2	4.240(2)
N1–Li1	2.28(2)	Ba2–Ba2	3.844(3)
Ba1–Li1 × 2	3.36(2)	Ba2–Ba2	4.136(3)
Ba1–Li1 × 2	3.59(2)	Ba2–Li1 × 2	3.31(2)
Ba1–Ba1	3.879(3)	Ba2–Li1 × 2	3.52(2)
Ba1–Ba1	4.101(3)		

same fashion as that of $NaBa_2O$ [20]. In both structures, double layers of Ba atoms are separated by single layers of either Na or Li atoms corresponding to the hypothetical alloys "$NaBa_2$" and "$LiBa_2$" with the $MoSi_2$-type [21] structure. The difference between the two constructions lies in the occupation of voids by O/N atoms. While in $NaBa_2O$ part of the tetrahedral voids in the double Ba layers are occupied, N atoms in $LiBa_2N$ fill octahedral voids surrounded each by one Li and five Ba atoms. It should be emphasized that so far one subnitride with both Ba–N and Li–N bonds had been found to exist [11]; however, no subnitride has been shown with Na–N bonds.

As mentioned above, there are two different Ba positions in the structure with close contacts with two and three N atoms. Ba–Ba and Ba–Li interatomic distances are in the ranges 3.844(3)–4.396(1) and 3.31(2)–3.59(2) Å, respectively, Ba–N distances are 2.69(1), 2.79(1), and 2.83(1) Å, all similar to those in other Li–Ba and Na–Ba subnitrides. Li–N bonds (2.28(2) Å) are a little longer than found in $Li_{80}Ba_{39}N_9$ [11] or Li_3N [22] ($d_{Li–N}$: 1.74–2.11 Å). In the structure of $LiBa_2N$ also two types of octahedral voids exist between parallel rows in one plane ($LiBa_5$) and between different planes (Li_2Ba_4), with $d_{Ba–Ba} = 3.992$ (1)–4.240(1) Å and $d_{Ba–Li} = 3.29(2)$–3.59(1) Å.

The X-ray powder diffractogram of the reaction product aimed at $LiBa_3N$ turned out to contain lines of $LiBa_3N$ together with those of Ba_2N. The calculated pattern assuming the atomic coordinates of $NaBa_3N$ was in good agreement with the main lines of the experimental pattern. Unfortunately, the samples with a high content of $LiBa_3N$ were very ductile and no single crystals could be extracted. The results of the indexing of the diffractogram are shown in Table 5. $LiBa_3N$ crystallizes in hexagonal symmetry with unit cell parameters $a = 8.182(1)$, $c = 6.922(4)$ Å (space group $P6_3/mmc$, $Z = 2$) (Fig. 3) and has the anti-type structure of $BaNiO_3$ [23].

The positional parameters for the $LiBa_3N$ and $NaBa_3N$ structures were optimized via total energy minimizations.

Table 5
Observed and calculated diffraction data for the $LiBa_3N$ compound ($BaNiO_3$[23] structure type, space group $P6_3/mmc$, Mo$K_{\alpha 1}$ radiation)

h	k	l	$2\theta_{obs}$	$2\theta_{calc}$	I_{obs}	I_{calc}
0	1	0	5.751	5.737	54.1	58.7
0	1	1	8.200	8.208	12.0	8.8
1	1	0	9.959	9.946	3.2	4.2
0	2	0	11.493	11.489	15.9	19.1
0	0	2	11.770	11.746	22.3	29.5
0	2	1	12.897	12.909	100	100
0	1	2	13.056	13.081	13.4	8.9
1	2	1	16.338[a]	16.180	32.1[b]	20.7
0	2	2		16.462		18.0
0	3	1	18.268	18.253	12.1	13.9
2	2	0	19.967	19.967	11.3	13.5
2	3	0	25.204	25.200	11.4	8.4
2	5	1	36.923	36.927	2.9	3.4

$R(I) = \Sigma|I_{obs} - I_{calc}|/\Sigma I_{calc} = 0.123$.
[a]Average angle.
[b]Summarized intensity for (1 2 1) and (0 2 2).

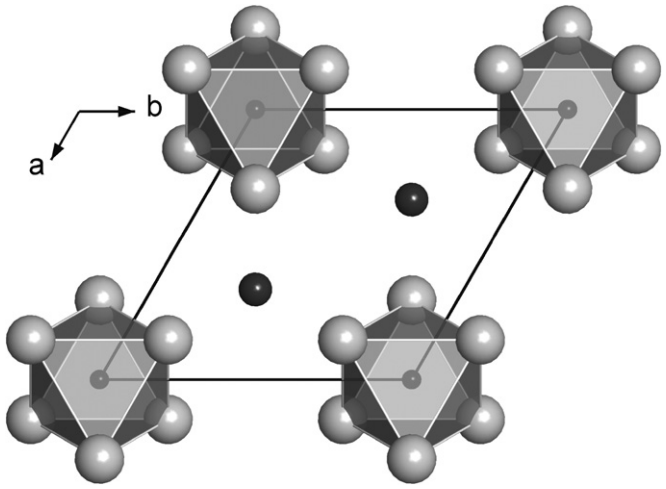

Fig. 3. Crystal structure of $LiBa_3N$.

Table 6
Experimental and theoretically optimized parameters (P) of Li(Na)Ba_3N

P	$NaBa_3N$	$LiBa_3N$	Δ, %
Experimental			
a, Å	8.4414(6)	8.182(1)	−3.1
c, Å	6.9817(8)	6.922(4)	−0.9
x(Ba)	0.1439(1)	—	—
$d_{Ba–N}$, Å	2.734(1)	2.722[a]	−0.44
Theoretical			
a, Å	8.47	8.22	−2.9
c, Å	6.95	6.88	−1.0
x(Ba)	0.1439	0.1483	—
$d_{Ba–N}$, Å	2.734	2.723	−0.40

[a]Based on the theoretical value for x(Ba). $\left(\Delta = \frac{P_{LiBa_3N} - P_{NaBa_3N}}{P_{NaBa_3N}} \times 100\%\right)$.

Table 7
Atomic coordinates for $LiBa_3N$

Atom	Position	x	y	z
Li	2*c*	1/3	2/3	1/4
Ba	6*h*	0.2966[a]	0.1483[a]	1/4
N	2*a*	0	0	0

[a]Taken from total energy optimization.

The results are compared with the experimental ones in Tables 6 and 7. The optimized c/a ratio for $NaBa_3N$ is somewhat lower than observed, while the unit cell volume and the x_{Ba} parameter are reproduced very well. Relative changes in the lattice constants from $NaBa_3N$ to $LiBa_3N$ are reproduced quite well too. The theoretical value of x_{Ba} for $LiBa_3N$ is quite reasonable when the Ba–N distances in the two compounds are compared. These theoretical results thus can be viewed as an argument in favor of the proposed structure and composition of $LiBa_3N$.

In view of the incorporation of both Ba and Li in the $LiBa_5N$ octahedron of the $LiBa_2N$ structure, the question

remains whether Li also partly substitutes the Ba_6N octahedra in $LiBa_3N$ in contrast to $NaBa_3N$ where Na stays entirely in the space between the Ba_3N chains. An answer to this question needs more detailed investigations. Preliminary investigations indicate the possibility of substituting the Li atoms by Na. One sample was prepared aiming at the composition $Li_{0.5}Na_{0.5}Ba_3N$. In the X-ray diagram a phase (Li,Na)Ba_3N was observed together with Ba_2N. The presence of an excess of Li is generally not observable. According to EDX analysis the atomic ratio Na/Ba in the compound was 1:4, which corresponds to $Li_{0.25}Na_{0.75}Ba_3N$. The powder diffractogram of the phase was indexed in hexagonal symmetry with unit cell parameters $a = 8.381(3)$, $c = 6.953(6)$ Å, a little smaller than these of $NaBa_3N$ ($a = 8.4414$, $c = 6.9817$ Å).

3.2. Thermal analysis

The decomposition temperature of $LiBa_3N$ (237 °C) is a little higher than that of $Li_{80}Ba_{39}N_9$ [11] (165 °C) and the two intermetallic Li–Ba compounds $BaLi_4$ [9] and $Ba_{19}Li_{44}$ [10] (156 and 126 °C, respectively), but lower than for $NaBa_3N$ (405 °C) [24] or Ba_3N (550 °C) [24]. According to powder X-ray analysis $LiBa_2N$ could only be identified as a minority phase (approx. 20%) in the preparation besides Ba_2N and $LiBa_3N$. Thermal analysis of such products did not indicate any effect except for the decomposition of $LiBa_3N$ (237 °C) in the temperature region up to 600 °C.

4. Summary

The metal-rich part of the Li–Ba–N system was investigated, and ternary subnitrides could be identified, including two new compounds, $LiBa_2N$ and $LiBa_3N$. These subnitrides were synthesized from the metals and barium azide and structurally characterized by single crystal and powder X-ray diffraction. The structure of $LiBa_2N$ contains perpendicular rows of edge-sharing $LiBa_5N$ octahedra. The structure of $LiBa_3N$ is made up from rows of face-sharing Ba_6N octahedra with Li atoms between them; however, a partial substitution of Ba by Li cannot be excluded. In contrast there is clear evidence that Li in $LiBa_3N$ can be substituted by Na, as demonstrated with the intermediate phase $Li_{0.25}Na_{0.75}Ba_3N$.

Appendix A. Supplementary data

Supplementary data associated with this article can be found in the online version at doi:10.1016/j.jssc.2007.04.012.

References

[1] A. Simon, in: M. Driess, H. Nöth, (Eds.), Molecular Clusters of the Main Group Elements, Wiley-VCH, Weinheim, 2004, pp. 246–266.
[2] O. Reckeweg, F. DiSalvo, Solid State Sci. 4 (2002) 575–584.
[3] P. Rauch, A. Simon, Angew. Chem. 104 (1992) 1505–1506.
[4] G. Snyder, A. Simon, J. Am. Chem. Soc. 117 (1995) 1996–1999.
[5] G. Snyder, A. Simon, Angew. Chem. 106 (1994) 713–715.
[6] A. Simon, U. Steinbrenner, J. Chem. Soc. Faraday Trans. 92 (1996) 2117–2123.
[7] G.V. Vajenine, A. Simon, Eur. J. Inorg. Chem. 2001 (2001) 1189–1193.
[8] G.V. Vajenine, U. Steinbrenner, A. Simon, C.R. Acad. Sci. Paris Ser. IIc 2 (1999) 583–589.
[9] V. Smetana, V. Babizhetskyy, C. Hoch, A. Simon, Z. Kristallogr. NCS 221 (2006) 434.
[10] V. Smetana, V. Babizhetskyy, G.V. Vajenine, C. Hoch, A. Simon, Inorg. Chem., accepted for publication.
[11] V. Smetana, V. Babizhetskyy, G.V. Vajenine, A. Simon, Inorg. Chem. 45 (2006) 10786–10789.
[12] A. Altomare, M. Burla, M. Camalli, B. Carroccini, G. Cascarano, C. Giacovazzo, A. Guagliardi, A. Moliterni, G. Polidori, R. Rizzi, J. Appl. Crystallogr. 32 (1999) 115.
[13] G.M. Sheldrick, *SHELXL-97:* Program for the Refinement of Crystal Structures, University of Göttingen, Germany, 1997.
[14] L. Farrugia, J. Appl. Crystallogr. 32 (1999) 837.
[15] L. Akselrud, P. Zavalii, Yu. Grin, V. Pecharsky, B. Baumgartner, E. Wölfel, Mater. Sci. Forum 133–136 (1993) 335–340.
[16] A. Simon, J. Appl. Crystallogr. 4 (1971) 138–145.
[17] P. Blaha, K. Schwarz, G.K.H. Madsen, D. Kvasnicka, J. Luitz, *WIEN2k*, An Augmented Plane Wave + Local Orbitals Program for Calculating Crystal Properties, Karlheinz Schwarz, Techn. Universität Wien, Austria, ISBN 3-9501031-1-2, 2001.
[18] J.P. Perdew, S. Burke, M. Ernzerhof, Phys. Rev. Lett. 77 (1996) 3865–3868.
[19] H. Weiss, G.V. Vajenine, U. Steinbrenner, A. Simon, E. Balthes, P Wyder, Phys. Rev. B 63 (2001) 115104-1–115104-8.
[20] G.V. Vajenine, A. Simon, Angew. Chem. 113 (2001) 4348–4351.
[21] Y. Harada, M. Morinaga, D. Saso, M. Takata, M. Sakata, Intermetallics 6 (1998) 523–527.
[22] H. Schulz, K. Schwarz, Acta Crystallogr. A 34 (1978) 999–1005.
[23] Y. Takeda, F. Kanamaru, M. Shimada, M. Koizumi, Acta Crystallogr. B 32 (1976) 2464–2466.
[24] U. Steinbrenner, Thesis, Stuttgart, Germany, 1997.